J|A|C|S
ARTICLES
Published on Web 01/26/2006

CNT−CdTe Versatile Donor−Acceptor Nanohybrids

Dirk M. Guldi,*,† G. M. Aminur Rahman,† Vito Sgobba,† Nicholas A. Kotov,‡ Davide Bonifazi,§ and Maurizio Prato*,§

Contribution from the Institute for Physical and Theoretical Chemistry, Universität Erlangen, 91058 Erlangen, Germany, Department of Chemical Engineering University of Michigan, Ann Arbor, Michigan 48109, and Dipartimento di Scienze Farmaceutiche, Università di Trieste, Piazzale Europa 1, Trieste 34127, Italy

Received July 27, 2005; E-mail: dirk.guldi@chemie.uni-erlangen.de; prato@univ.trieste.it

Abstract: Single wall carbon nanotubes (SWNT) and multiwall carbon nanotubes (MWNT) were linked to thioglycolic acid (TGA)-capped CdTe nanoparticles (NP) through electrostatic interactions producing photoactive superstructures. The novel nanohybrids were characterized both in the ground and excited states with specific accent on electron-transfer chemistry. In fact, both assays provide kinetic and spectroscopic evidence that support a partial transfer of charge density, with rapid formation of microsecond-lived radical ion pair states. Since nanotubes provide a quick transportation route of charge carriers to the electrode, we took this remarkable finding further and constructed photoelectrochemical cells. Photocurrents were generated through the implementation of CdTe and SWNT or MWNT, which serve as excited-state electron donor components and electron acceptors, respectively.

Introduction

In recent years, the integration of organic and inorganic building blocks into novel nanohybrid structures has drawn a broad interdisciplinary attention,[1] as this approach to innovative materials bears interesting opportunities for the control over fine-tuning desirable functionalities.[2] In the continuous search for suitable systems useful in photovoltaics, electron donor−acceptor arrays are particularly promising.[3,4] In this context, the interactions between the components play an important role. Relevant aspects include (i) solubility,[5] (ii) optimizing the frontier orbital energy levels and offsets of donors and acceptors,[6] (iii) improving the absorption cross section/solar light harvesting,[7] (iv) stabilizing radical ion pair states,[5d,8] (v) optimizing the layer and interface morphologies,[2c,6f,9] and (vi) fine-tuning the charge carrier mobilities.[10]

† Universität Erlangen.
‡ University of Michigan.
§ Università di Trieste.

(1) (a) *Host−Guest-Systems Based on Nanoporous Crystals*; Laeri, F., Schüth, F., Ulrich, S., Wark, M., Eds.; Wiley-VCH: Weinheim, Germany, 2003. (b) *Functional Hybrid Materials*; Gómez-Romero, P., Sanchez, C., Eds.; Wiley-VCH: Weinheim, Germany, 2003. (c) *Handbook of Organic−Inorganic Hybrid Materials and Nanocomposites*; Nalwa, H. S., Ed.; Hitachi Research Laboratory, Hitachi Ltd.: Japan, 2003. (d) Förster, S.; Plantenberg, T. *Angew. Chem., Int. Ed.* **2002**, *41*, 688−714. (e) Choy, J.-H. *J. Phys. Chem. Solids* **2004**, *65*, 373−383. (f) Choy, J. H.; Kwon, S. J.; Park, G. S. *Science* **1998**, *280*, 1589. (g) Smarsly, B.; Kaper, H. *Angew. Chem., Int. Ed.* **2005**, *44*, 3809−3811. (h) Mann, S.; Colfen, H. *Angew. Chem., Int. Ed.* **2003**, *42*, 2350−2365. (i) Agrawal, S., Kumar, A.; Frederick, M. J.; Ramanath, G. *Small* **2005**, *1*, 823−826. (j) Huynh, W. U.; Dittmer, J. J.; Alivisatos, A. P. *Science* **2002**, *295*, 2425−2427. (k) Bach, U.; Lupo, D.; Comte, P.; Moser, J. E.; Weissortel, F.; Salbeck, J.; Spreitzer, H.; Grätzel, M. *Nature* **1998**, *395*, 583−5. (l) Yu, W.; Zheng, X.; Feng, T.; Yang, S.; Lei, Q.; Qu, C.; Quan, S.; Xu, X. *Displays* **2004**, *25*, 61−65. (m) Rahman, G. M. A.; Guldi, D. M.; Zambon, E.; Pasquato, L.; Tagmatarchis, N.; Prato, M. *Small* **2005**, *1*, 527−530. (n) Luo, C.; Guldi, D. M.; Maggini, M.; Manna, E.; Mondini, S.; Kotov, N. A.; Prato, M. *Angew. Chem., Int. Ed.* **2000**, *39*, 3905−3909. (o) Lee, J.; Govorov, A. O.; Dulka, J.; Kotov, N. A. *Nano Lett.* **2004,** *4*, 2323. (p) Lee, J.; Govorov, A. O.; Kotov, N. A. *Angew. Chem., Int. Ed.* **2005**, *44*, 7439−7442.

(2) (a) *Photochemical Conversion and Storage of Solar Energy*; Pelizzetti, E., Schiavello, M., Eds.; Kluwer: Dordrecht, The Netherlands, 1997. (b) Nelson, J. *The Physics of Solar Cells (Properties of Semiconductor Materials)*; Imperial College Press: London, 2003. (c) *Organic Photovoltaics: Concepts and Realization*; Brabec, C., Dyakonov, V., Parisi, J., Sariciftci, S., Eds.; Springer Series in Materials Science; Springer: Berlin, 2003.

(3) (a) Sorescu, D. C.; Jordan, K. D.; Avouris, P. *J. Phys. Chem. B* **2001**, *105*, 11227. (b) Javey, A.; Guo, J.; Wang, Q.; Lundstrom, M.; Dai, H. J. *Nature* **2003**, *424*, 654. (c) Hegfeldt, A.; Grätzel, M. *Acc. Chem. Res.* **2000**, *33*, 269. (d) Grätzel, M. *Nature* **2001**, *414*, 338. (e) Bignozzi, C. A.; Argazzi, R.; Kleverlaan, C. J. *Chem. Soc. Rev.* **2000**, *29*, 87. (f) Halls, J. J. M.; Walsh, C. A.; Greenham, N. C.; Marseglia, E. A.; Friend, R. H.; Morati, S. C.; Holmes, A. B. *Nature* **1995**, *376*, 498. (g) Schmidt-Mende, L.; Fechtenkötter, A.; Müllen, K.; Moons, E.; Friend, R. H.; MacKenzie, J. D. *Science* **2001**, *295*, 2425.

(4) (a) Garnier, F. *J. Opt. A: Pure Appl. Opt.* **2002**, *4*, S247−S251. (b) Sargent, E. H. *Adv. Mater.* **2005**, *17*, 515−522. (c) Coe-Sullivan, S.; Woo, W. K.; Steckel, J. S.; Bawendi, M.; Bulovic, V. *Org. Electron.* **2003**, *4*, 123−130. (d) Sanchez, C.; Soler-Illia, G. J. De A. A.; Ribot, F.; Grosso, D. *C. R. Chim.* **2003**, *6*, 1131−1151. (e) Qian, G.; Guo, J.; Wang, M.; Si, J.; Qiu, J.; Hirao, K. *Appl. Phys. Lett.* **2003**, *83*, 2327−2329. (f) Walling, H. A.; Artzi, R.; Gwinn, E. G.; Naaman, R.; Maranowski, K.; Gossard, A. C. *Solid State Commun.* **2003**, *127*, 707−711. (g) Huang, X.; Li, J.; Zhang, Y.; Mascarenhas, A. *J. Am. Chem. Soc.* **2003**, *125*, 7049−7055. (h) Carlos, L. D.; Sa Ferreira, R. A.; Rainho, J. P.; De Zea Bermudez, V. *Adv. Funct. Mater.* **2002**, *12*, 819−823. (i) Megelski, S.; Calzaferri, G. *Adv. Funct. Mater.* **2001**, *11*, 277−286. (j) Baron, R.; Huang, C. H.; Bassani, D. M.; Onopriyenko, A.; Zayats, M.; Willner, I. *Angew. Chem., Int. Ed.* **2005**, *44*, 4010−4015. (k) Sheeney-Hay-Ichia, L.; Basnar, B.; Willner, I. *Angew. Chem., Int. Ed.* **2004**, *43*, 78−83. (l) Sheeney-Hay-Ichia, L.; Pogorelova, S.; Gofer, Y.; Willner, I. *Adv. Funct. Mater.* **2004**, *14*, 416−424. (m) Granot, E.; Patolsky, F.; Itamar, W. *J. Phys. Chem. B* **2004**, *108*, 5875−5881.

(5) (a) Skotheim, T. A.; Elsenbauer, R. L.; Reynolds, J. R. *Handbook of Conducting Polymers*; Marcel Dekker: New York, 1998. (b) Kim, Y.; Choulis, S. A.; Nelson, J.; Bradley, D. D. C.; Cook, S.; Durrant, J. R. *Appl. Phys. Lett.* **2005**, *86*, 063502/1−063502/3. (c) Nierengarten, J.-F. *New J. Chem.* **2004**, *28*, 1177−1191. (d) Tasis, D.; Tagmatarchis, N.; Georgakilas, V.; Prato, M. *Chem. Eur. J.* **2003**, *9*, 4000−4008. (e) Qin, S.; Qin, D.; Ford, W. T.; Herrera, J. E.; Resasco, D. E.; Bachilo, S. M.; Weisman, R. B. *Macromolecules* **2004**, *35*, 3965.

(6) (a) Sun, S.-S. *Sol. Energy Mater. Sol. Cells* **2004**, *85*, 261−267. (b) Sun, S.-S. *Mater. Sci. Eng., B* **2005**, *116*, 251−256. (c) Nelson, J.; Kirkpatrick, J.; Ravirajan, P. *Phys. Rev. B: Condens. Matter Mater. Phys.* **2004**, *69*, 035337/1−035337/11. (d) Lemaur, V.; Steel, M.; Beljonne, D.; Bredas, J.-L.; Cornil, J. *J. Am. Chem. Soc.* **2005**, *127*, 6077−6086. (e) Peumans, P.; Forrest, S. R. *Chem. Phys. Lett.* **2004**, *398*, 27−31. (f) Sylvester-Hvid, K. O.; Ratner, M. A. *J. Phys. Chem. B* **2005**, *109*, 200−208.

Carbon nanotubes (CNT) and especially single wall carbon nanotubes (SWNT) fit perfectly into this picture.[11] They are hexagonal networks of carbon atoms, rolled up to create seamless cylinders. These carbon tubes can reach lengths of centimeters, and each end is usually capped with half of a fullerene sphere. Several key challenges arise around these nanostructured carbon allotropes. Can these quasi one-dimensional superstructures serve donor or acceptor functions in novel nanohybrids? Does the exceptional conductivity along the tubular axis in CNT lead to new paradigms in electron-transfer chemistry? Equally intriguing are multiwall carbon nanotubes (MWNT), in which the presence of numerous concentric cylinders provides different acceptor levels.[12]

Recently, the first reports on all organic donor−acceptor nanohybrids appeared, combining CNT with either polymeric components or metalloporphyrins.[5d,12a,c,13] Work performed either in condensed media or at electrode surfaces demonstrated that the presence of extended, delocalized π-electron systems is, indeed, very useful in terms of charge transfer and charge transport.[5a,11a,14] For example, illuminating CNT-based donor−acceptor nanohybrids with visible light is followed by fast charge separation and slow charge recombination. The lifetimes of the charge-separated radical ion pair state are so long that these systems can be used for the fabrication of photovoltaic devices. However, little is known about these nanoparticle−nanotube hybrids, which led us to concentrate in the current work on combining CNT with differently sized water-soluble nanoparticles, namely, red- and green-emitting CdTe[14] (i.e., 5.0 and 2.4 nm)—see for illustration Scheme 1.

(7) (a) Subramanian, V.; Evans, D. G. *J. Phys. Chem. B* **2004**, *108*, 1085−1095. (b) Loewe, R. S.; Tomizaki, K.; Youngblood, W. J.; Bo, Z.; Lindsey, J. S. *J. Mater. Chem.* **2002**, *12*, 3438−3451. (c) Chen, Y.; Zeng, Z.; Li, Chao; Wang, W.; Wang, X.; Zhang, B. *New J. Chem.* **2005**, *29*, 773−776. (d) Amao, Y.; Yamada, Y. *Langmuir* **2005**, *21*, 3008−3012. (e) Wang, P.; Klein, C.; Humphry-Baker, R.; Zakeeruddin, S. M.; Graetzel, M. *J. Am. Chem. Soc*. **2005**, *127*, 808−809.

(8) (a) Mikhelashvili, M. S.; Agam, O. *J. Lumin.* **2005**, *114*, 145−154. (b) Beek, W. J. E.; Wienk, M. M.; Kemerink, M.; Yang, X.; Janssen, R. A. J. *J. Phys. Chem. B* **2005**, *109*, 9505−9516. (c) Sanchez, L.; Sierra, M.; Martin, N.; Guldi, D. M.; Wienk, M. W.; Janssen, R. A. J. *Org. Lett.* **2005**, *7*, 1691−1694. (d) Kanato, H.; Takimiya, K.; Otsubo, T.; Aso, Y.; Nakamura, T.; Araki, Y.; Ito, O. *J. Org. Chem.* **2004**, *69*, 7183−7189. (e) Okamoto, K.; Fukuzumi, S. *J. Phys. Chem. B* **2005**, *109*, 7713−7723. (f) Sessler, J. L.; Jayawickramarajah, J.; Gouloumis, A.; Torres, T.; Guldi, D. M.; Maldonado, S.; Stevenson, K. J. *Chem. Commun.* **2005**, 1892−1894. (g) Han, Y.; Dobeck, L.; Gong, A.; Meng, F.; Spangler, C. W.; Spangler, L. H. *Chem. Commun.* **2005**, 1067−1069. (h) Imahori, H.; Sekiguchi, Y.; Kashiwagi, Y.; Sato, T.; Araki, Y.; Ito, O.; Yamada, H.; Fukuzumi, S. *Chem. Eur. J.* **2004**, *10*, 3184−3196. (i) Miyamoto, N.; Kuroda, K.; Ogawa, M. *J. Phys. Chem. B* **2004**, *108*, 4268−4274. (j) Ohkubo, K.; Kotani, H.; Shao, J.; Ou, Z.; Kadish, K. M.; Li, G.; Pandey, R. K.; Fujitsuka, M.; Ito, O.; Imahori, H.; Fukuzumi, S. *Angew. Chem., Int. Ed.* **2004**, *43*, 853−856. (k) Fukuzumi, S.; Ohkubo, K.; Wenbo, E.; Ou, Z.; Shao, J.; Kadish, K. M.; Hutchison, J. A.; Ghiggino, K. P.; Sintic, P. J.; Crossley, M. J. *J. Am. Chem. Soc*. **2003**, *125*, 14984−14985. (l) Kashiwagi, Y.; Ohkubo, K.; McDonald, J. A.; Blake, I. M.; Crossley, M. J.; Araki, Y.; Ito, O.; Imahori, H.; Fukuzumi, S. *Org. Lett.* **2003**, *5*, 2719−2721. (m) Loi, M. A.; Denk, P.; Hoppe, H.; Neugebauer, H.; Winder, C.; Meissner, D.; Brabec, C.; Sariciftci, N. S.; Gouloumis, A.; Vazquez, P.; Torres, T. *J. Mater. Chem.* **2003**, *13*, 700−704. (n) Burley, G. A.; Avent, A. G.; Boltalina, O. V.; Gol'dt, I. V.; Guldi, D. M.; Marcaccio, M.; Paolucci, F.; Paolucci, D.; Taylor, R. *Chem. Commun.* **2003**, 148−149.

(9) (a) Liu, J.; Kadnikova, E. N.; Liu, Y.; McGehee, M. D.; Frechet, J. M. J. *J. Am. Chem. Soc*. **2004**, *126*, 9486−9487. (b) Al-Ibrahim, M.; Ambacher, O.; Sensfuss, S.; Gobsch, G. *Appl. Phys. Lett*. **2005**, *86*, 201120/1−201120/3. (c) Kim, Y.; Choulis, S. A.; Nelson, J.; Bradley, D. D. C.; Cook, S.; Durrant, J. R. *J. Mater. Sci.* **2005**, *40*, 1371−1376. (d) Kim, Y.; Choulis, S. A.; Nelson, J.; Bradley, D. D. C.; Cook, S.; Durrant, J. R. *Appl. Phys. Lett.* **2005**, *86*, 063502/1−063502/3. (e) Shen, Q.; Arae, D.; Toyoda, T. *J. Photochem. Photobiol., A* **2004**, *164*, 75−80. (f) Sirimanne, P. M.; Tributsch, H. *J. Solid State Chem.* **2004**, *177*, 1789−1795. (g) Mayer, A. C.; Lloyd, M. T.; Herman, D. J.; Kasen, T. G.; Malliaras, G. G. *Appl. Phys. Lett.* **2004**, *85*, 6272−6274. (h) Chirvase, D.; Parisi, J.; Hummelen, J. C.; Dyakonov, V. *Nanotechnology* **2004**, *15*, 1317−1323. (i) Moons, E. *J. Phys.: Condens. Matter* **2002**, *14*, 12235−12260. (j) Nierengarten, J.-F.; Eckert, J.-F.; Felder, D.; Nicoud, J.-F.; Armaroli, N.; Marconi, G.; Vicinelli, V.; Boudon, C.; Gisselbrecht, J.-P.; Gross, M.; Hadziioannou, G.; Krasnikov, V.; Ouali, L.; Echegoyen, L.; Liu, S.-G. *Carbon* **2000**, *38*, 1587−1598. (k) Haerter, J. O.; Chasteen, S. V.; Carter, S. A.; Scott, J. C. *Appl. Phys. Lett*. **2005**, *86*, 164101/1−164101/3. (l) Yang, X.; Loos, J.; Veenstra, S. C.; Verhees, W. J. H.; Wienk, M. M.; Kroon, J. M.; Michels, M. A. J.; Janssen, R. A. J. *Nano Lett.* **2005**, *5*, 579−583. (m) Cass, M. J.; Walker, A. B.; Martinez, D.; Peter, L. M. *J. Phys. Chem. B* **2005**, *109*, 5100−5107. (n) Drees, M.; Davis, R. M.; Heflin, J. R. *J. Appl. Phys*. **2005**, *97*, 036103/1−036103/3. (o) Snaith, H. J.; Greenham, N. C.; Friend, R. H. *Adv. Mater.* **2004**, *16*, 1640−1645. (p) Hoppe, H.; Niggemann, M.; Winder, C.; Kraut, J.; Hiesgen, R.; Hinsch, A.; Meissner, D.; Sariciftci, N. S. *Adv. Funct. Mater.* **2004**, *14*, 1005−1011. (q) Roberson, L. B.; Poggi, M. A.; Kowalik, J.; Smestad, G. P.; Bottomley, L. A.; Tolbert, L. M. *Coord. Chem. Rev.* **2004**, *248*, 1491−1499. (r) Schroeder, R.; Ullrich, B. *Appl. Phys. Lett.* **2002**, *81*, 556−558.

(10) (a) Chen, F.-C.; Xu, Q.; Yang, Y. *Appl. Phys. Lett.* **2004**, *84*, 3181−3183. (b) Chen, S.-G.; Stradins, P.; Gregg, B. A. *J. Phys. Chem. B* **2005**, *109*, 13451−13460. (c) Gregg, B. A.; Chen, S.-G.; Cormier, R. A. *Chem. Mater.* **2004**, *16*, 4586−4599. (d) Gregg, B. A. *J. Phys. Chem. B* **2003**, *107*, 4688−4698. (e) Pasimeni, L.; Franco, L.; Ruzzi, M.; Mucci, A.; Schenetti, L.; Luo, C.; Guldi, D. M.; Kordatos, K.; Prato, M. *J. Mater. Chem.* **2001**, *11*, 981−983.

(11) (a) *One-Dimensional Metal Conjugated Polymers, Organic Crystals, Carbon Nanotubes*; Roth, S., Carroll, D., Eds.; Wiley-VCH: Weinheim, Germany, 2004. (b) *Introduction to Nanotechnology*; Poole, C. P., Owens, F. J., Eds.; Wiley-Interscience: Weinheim, Germany, 2003. (c) *Nanophysics and Nanotechnology: An Introduction to Modern Concepts in Nanoscience*; Wolf, E. L., Ed.; John Wiley & Sons: New York, 2004. (d) Rao, C. *Chemistry of Nanomaterials: Synthesis, Properties and Applications*; Wiley-VCH: Weinheim, Germany, 2004. (e) Cao, G. *Nanostructures and Nanomaterials: Synthesis, Properties & Applications*; Imperial College Press: London, 2004. (f) *Carbon Nanotubes and Related Structures: New Materials for the Twenty-First Century*; Harris, P., Ed.; Cambridge University Press: Cambridge, 2001. (g) *Carbon Nanotubes: Synthesis, Structure, Properties and Applications*; Dresselhaus, M. S., Dresselhaus, G., Avouris, P., Eds.; Springer: Berlin, 2001. (h) Reich, S.; Thomsen, C.; Maultzsch, J. *Carbon Nanotubes: Basic Concepts and Physical Properties*; VCH: Weinheim, Germany, 2004. (i) Special Issue on Carbon Nanotubes. *Acc. Chem. Res.* **2002**, *35*, 997−1113. (j) Guldi, D. M. *J. Phys. Chem. B* **2005**, *109*, 11432−11441. (k) Gooding, J. J. *Electrochim. Acta* **2005**, *50*, 3049−3060. (l) Bellucci, S. *Phys. Status Solidi C* **2005**, *2*, 34−47. (m) Banerjee, S.; Hemraj-Benny, T.; Wong, S. S, *Adv. Mater.* **2005**, *17*, 17−29. (n) Bianco, A.; Kostarelos, K.; Partidos, C. D.; Prato, M. *Chem. Commun.* **2005**, 571−577. (o) Dyke, C. A.; Tour, J. M. *J. Phys. Chem. A* **2004**, *108*, 11151−11159. (p) Katz, E.; Willner, I. *Chem. Phys. Chem.* **2004**, *5*, 1084−1104. (q) Dresselhaus, M. S.; Dresselhaus, G.; Jorio, A. *Annu. Rev. Mater. Res.* **2004**, *34*, 247−278. (r) Ciraci, S.; Dag, S.; Yildirim, T.; Guelseren, O.; Senger, R. T. *J. Phys.: Condens. Matter* **2004**, *16*, R901−R960. (s) Duerkop, T.; Kim, B. M.; Fuhrer, M. S. *J. Phys.: Condens. Matter* **2004**, *16*, R553−R580. (t) Lin, Y.; Taylor, S.; Li, H.; Fernando, K. A. S.; Qu, L.; Wang, W.; Gu, L.; Zhou, B.; Sun, Y.-P. *J. Mater. Chem.* **2004**, *14*, 527−541. (u) Tagmatarchis, N.; Prato, M. *J. Mater. Chem.* **2004**, *14*, 437−439. (v) Hirsch, A. *Angew. Chem., Int. Ed.* **2002**, *41*, 1853. (w) Bahr, J. L.; Tour, J. M. *J. Mater. Chem.* **2002**, *12*, 1952. (x) Banerjee, S.; Kahn, M. G. C.; Wang, S. S. *Chem. Eur. J.* **2003**, *9*, 1898. (y) Dyke, C. A.; Tour, J. M. *Chem. Eur. J.* **2004**, *10*. 812.

(12) (a) Guldi, D. M.; Rahman, G. M. A.; Jux, N.; Balbinot, D.; Tagmatarchis, N.; Prato, M. *Chem. Commun.* **2005**, 2038−2040. (b) Ago, H.; Petrisch, K.; Shaffer, M. S. P.; Windle, A. H.; Friend, R. H. *Adv. Mater.* **1999**, *11*, 1281−1285. (c) Qu, J.; Shen, Y.; Qu, X.; Dong, S. *Electroanalysis* **2004**, *16*, 1444−1450. (d) Wu, F. H.; Zhao, G. C.; Wei, X. W. *Electrochem. Commun.* **2002**, *4*, 690−693. (e) Li, J.; Cassell, A.; Delzeit, L.; Han, J.; Meyyappan, M. *J. Phys. Chem. B* **2002**, *106*, 9299−9305.

(13) (a) Guldi, D. M.; Taieb, H.; Rahman, G. M. A.; Tagmatarchis, N.; Prato, M. *Adv. Mater.* **2005**, *17*, 871−875. (b) Baskaran, D.; Mays, J. W.; Zhang, X. P.; Bratcher, M. S. *J. Am. Chem. Soc.* **2005**, *127*, 6916−6917. (c) Guldi, D. M.; Rahman, G. M. A.; Prato, M.; Jux, N.; Qin, S.; Ford, W. *Angew. Chem., Int. Ed.* **2005**, *44*, 2015−2018. (d) Chen, J.; Collier, C. P. *J. Phys. Chem. B* **2005**, *109*, 7605−7609. (e) Satake, A.; Miyajima, Y.; Kobuke, Y. *Chem. Mater.* **2005**, *17*, 716−724. (f) Guldi, D. M.; Rahman, G. M. A.; Jux, N.; Tagmatarchis, N.; Prato, M. *Angew. Chem., Int. Ed.* **2004**, *43*, 5526−5530. (g) Li, H.; Martin, R. B.; Harruff, B. A.; Carino, R. A.; Allard, L. F.; Sun, Y.-P. *Adv. Mater.* **2004**, *16*, 896−900. (h) Murakami, H.; Nomura, T.; Nakashima, N. *Chem. Phys. Lett.* **2003**, *378*, 481−485. (i) Bhattacharyya, S.; Kymakis, E.; Amaratunga, G. A. J. *Chem. Mater.* **2004**, *16* (23), 4819. (j) Guldi, D. M.; Rahman, G. M. A.; Ramey, J.; Marcaccio, M.; Paolucci, D.; Paolucci, F.; Qin, S.; Ford, W. T.; Balbinot, D.; Jux, N.; Tagmatarchis, N.; Prato, M. *Chem. Commun.* **2004**, 2034−2035. (k) Rahman, G. M. A.; Guldi, D. M.; Cagnoli, R.; Mucci, A.; Schenetti, L.; Vaccari, L.; Prato, M. *J. Am. Chem. Soc.* **2005**, *127*, 10051.

(14) (a) Weiss, E. A.; Ahrens, M. J.; Sinks, L. E.; Gusev, A. V.; Ratner, M. A.; Wasielewski, M. R. *J. Am. Chem. Soc.* **2004**, *126*, 5577−5584. (b) Nitzan, A.; Ratner, M. A. *Science* **2003**, *300*, 1384−1389. (c) Davis, W. B.; Svec, W. A.; Ratner, M. A.; Wasielewski, M. R. *Nature* **1998**, *396*, 60−63. (d) Robertson, N.; McGowan, C. A. *Chem. Soc. Rev.* **2003**, *32*, 96−103. (e) Egger, R.; Gogolin, A. O. *Chem. Phys.* **2002**, *281*, 447−454. (f) Xue, Y.; Ratner, M. A. *Nanotechnology* **2005**, *16*, 5−9. (g) Balasubramanian, K.; Burghard, M.; Kern, K.; Scolari, M.; Mews, A. *Nano Lett.* **2005**, *5*, 507−510. (h) Yang, X.; Chen, L.; Shuai, Z.; Liu, Y.; Zhu, D. *Adv. Funct. Mater.* **2004**, *14*, 289−295. (i) Stafstrom, S.; Hansson, A.; Johansson, A. *Synth. Met.* **2003**, *137*, 1397−1399.

Scheme 1. Partial Structure of the SWNT/Pyrene$^+$/CdTe Used in This Work

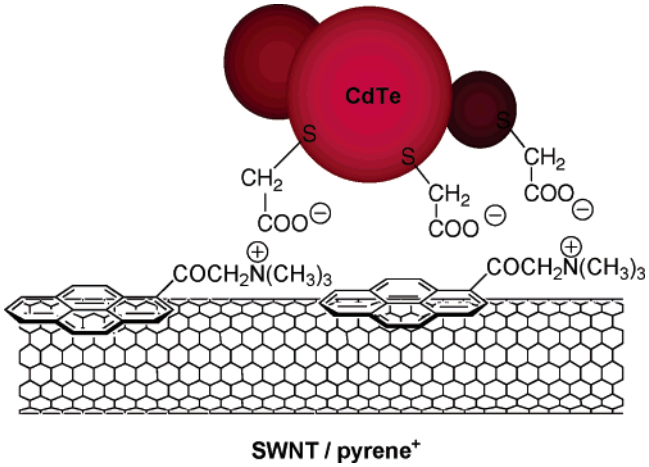

Results and Discussion

En route toward novel organic–inorganic nanohybrids we followed a strategy that is based on binding CNT and CdTe through electrostatic interactions and layer-by-layer assembly.[16] Details on the preparation of the CNT templates (i.e., SWNT/pyrene$^+$, MWNT/pyrene$^+$, SWNT/pyrene$^-$, and MWNT/pyrene$^-$) have been reported elsewhere.[17] Important is that our approach guarantees (i) significant debundling into individual CNT and (ii) formation of stable suspensions, for example, in water. Furthermore, the presence of trimethylammonium groups in pyrene$^+$ allows their association with negatively charged headgroups, present in thioglycolic acid (TGA)-stabilized size-quantized CdTe nanoparticles, to yield novel CNT/CdTe nanoassemblies. To probe such interactions we titrated aqueous solutions of CdTe with variable concentrations of SWNT/pyrene$^+$ or MWNT/pyrene$^+$ and monitored changes in the characteristic band gap transitions of CdTe—both in absorption and luminescence. In absorption (see Figure S1 in the Supporting Information), during the titration the features of CNT unequivocally emerge, especially the classical van Hove singularities of SWNT, which extend throughout the near-infrared region. A consistent trend in all of these titration experiments is a shift of the CdTe absorption edge/peak toward higher transition energies reaching a few nanometers, despite the presence of the CNT-centered van Hove singularities. In luminescence experiments,

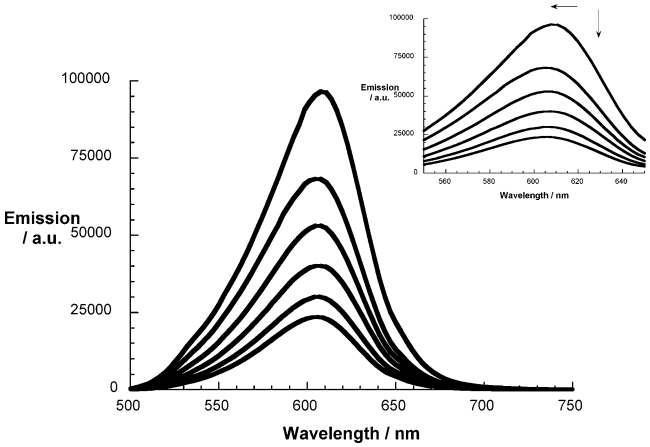

Figure 1. Room-temperature luminescence spectra of red-emitting CdTe, 5 nm, (1.5×10^{-6} M) upon addition of several concentrations of SWNT/pyrene$^+$ (0–0.2 mg/mL). The excitation wavelength is 350 nm, where the absorption of CdTe varies between 100% (i.e., 0 mg/mL SWNT/pyrene$^+$) and 75% (i.e., 0 mg/mL SWNT/pyrene$^+$); the luminescence spectra are, however, corrected for this effect. The inset shows an amplification of the 550–650 nm range.

quantum yields of 15–30% were determined in the absence of CNT,[16] and at different concentrations of SWNT/pyrene$^+$, excitation at 350 nm leads to nonlinear quenching effects of the strong CdTe-centered (1.5×10^{-6} M at pH 10.1) emission (Figure 1). Strong electronic interactions, such as transfer of charge density between the electroactive components, are likely to be responsible for the aforementioned effects (i.e., blue-shift and luminescence quenching). The binding constant is assumed—based on our previous work—as 10^5 M^{-1}.[16] These interactions can be potentially mediated by pyrene moieties.

The scope of a series of control experiments was to interfere with and/or to fine-tune the CNT/CdTe interactions. The protonation of TGA constitutes a simple and elegant means to manipulate the electrostatically driven formation of CNT/CdTe nanohybrids. Under slightly acidic conditions (pH < 6) protonating the carboxylate groups of the TGA, none of the above effects were noted. The absorption spectra, for example, are best described as linear combinations of the individual components (i.e., CdTe, ~590 nm; SWNT, metallic E_{11} transitions in the 500–600 nm range and semiconductor E_{22} and E_{11} transitions in the 600–900 nm/1000–1500 nm regions). The emission spectra after the 350 nm excitation display some quenching of CdTe luminescence, which originates, however, from competitive light absorption. Additional evidence for the dominant role of donor–acceptor process comes from control experiments involving similarly charged CdTe and CNT, which lead to negligible effects. For example, when probing SWNT/pyrene$^-$ and MWNT/pyrene$^-$,[17c] the presence of equally charged headgroups, namely, carboxylic acid, should prohibit meaningful CNT/CdTe interactions by electrostatic repulsion. In fact, the lack of appreciable blue-shifts or strong CdTe emission quenching, as observed in these cases (see Figure S2 in the Supporting Information) supports this notion. A similar conclusion stems from pyrene$^+$ and CdTe reference experiments.

In time-resolved emission experiments, we see lifetimes of around 6.5 ± 0.5 ns for red- and green-emitting CdTe in aerated aqueous solutions. Upon adding SWNT/pyrene$^+$ or MWNT/pyrene$^+$, within our time resolution, we see only the same long-lived component at, however, a much reduced amplitude. From

(15) (a) *Nanoparticles in Solids and Solutions*; Kamat, P. V., Meisel, D., Eds.; Kluwer: Dordrecht, The Netherlands, 1996. (b) *Semiconductor Nanoclusters*; Fendler, J. H., Ed.; Elsevier: Amsterdam, 1997. (c) *Nanoparticles: from Theory to Applications*; Schmid, G., Ed.; Wiley-VCH: Weinheim, Germany, 2004. (d) Rogach, A. L.; Katsikas, L.; Kornowski, A.; Su, D.; Eychmueller, A.; Weller, H. *Ber. Bunsen-Ges.* **1996**, *100*, 1772–1778. (e) Gao, M.; Rogach, A. L.; Kornowski, A.; Kirstein, S.; Eychmueller, A.; Mohwald, H.; Weller, H. *J. Phys. Chem. B* **1998**, *102*, 8360–8363. (f) Kapitonov, A. M.; Stupak, A. P.; Gaponenko, S. V.; Petrov, E. P.; Rogach A. L.; Eychmueller, A. *J. Phys. Chem. B* **1999**, *103*, 10109–10113. (g) Talapin, D. V.; Haubold, S.; Rogach, A. L.; Kornowski, A.; Haase, M.; Weller, H. *J. Phys. Chem. B* **2001**, *105*, 2260. (h) Mamedov, A. A.; Belov, A.; Giersig, M.; Mamedova, N. N.; Kotov, N. A. *J. Am. Chem. Soc.* **2001**, *123*, 7738–7739.

(16) (a) Guldi, D. M.; Zilbermann, I.; Anderson, G.; Kotov, N. A.; Tagmatarchis, N.; Prato, M. *J. Am. Chem. Soc.* **2004**, *126*, 14340–14341. (b) Guldi, D. M.; Zilbermann, I.; Anderson, G.; Kotov, N. A.; Tagmatarchis, N.; Prato, M. *J. Mater. Chem.* **2005**, *15*, 114–118. (c) Guldi, D. M.; Prato, M. *Chem. Commun.* **2004**, 2–10.

(17) (a) Nakashima, N.; Tomonari, Y.; Murakami, H. *Chem. Lett.* **2002**, 638–639. (b) Artyukhin, A. B.; Bakajin, O.; Stroeve, P.; Noy, A. *Langmuir* **2004**, *20*, 1442–1445. (c) Guldi, D. M.; Rahman, G. M. A.; Jux, N.; Balbinot, D.; Hartnagel, U.; Tagmatarchis, N.; Prato, M. *J. Am. Chem. Soc.* **2005**, *127*, 9830.

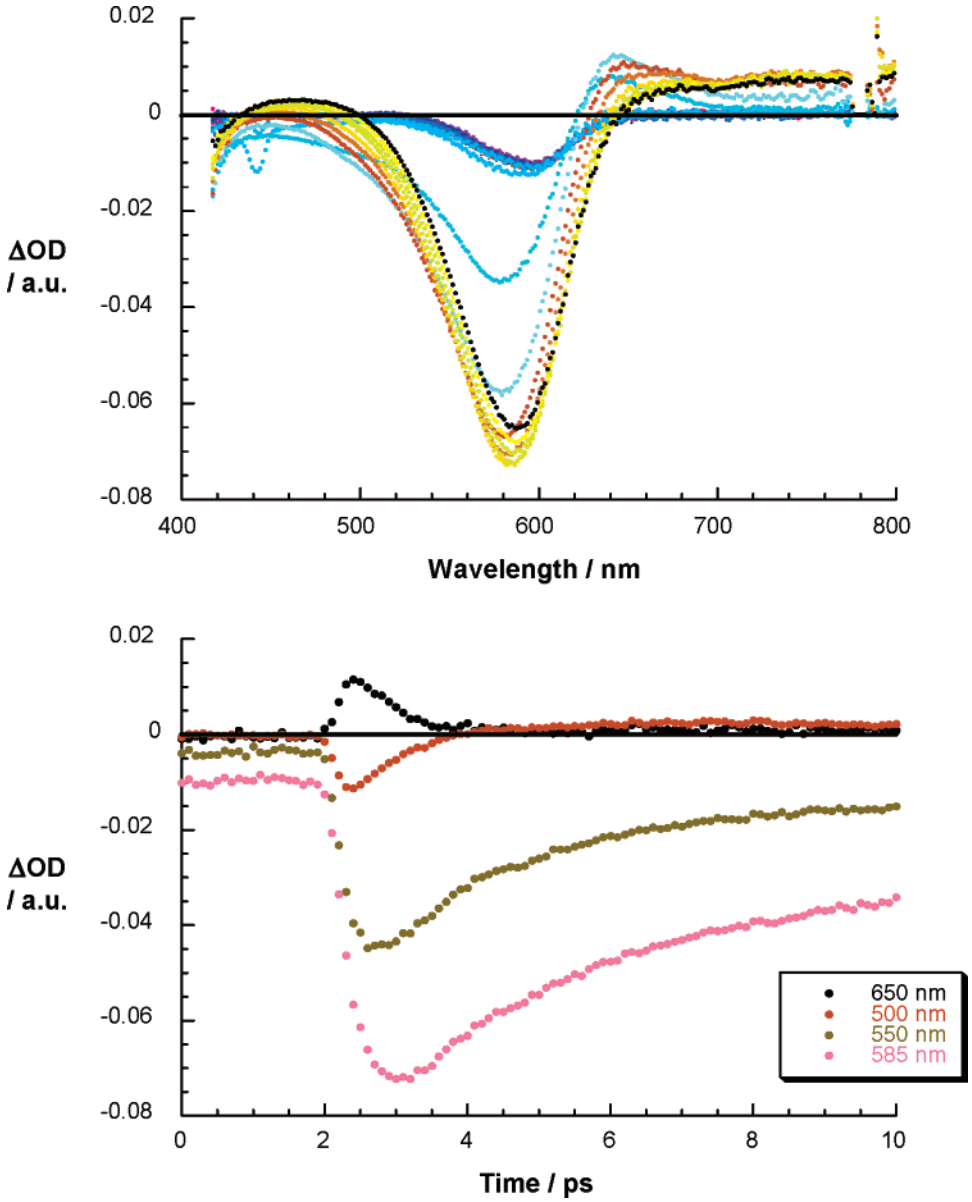

Figure 2. Upper part: differential absorption spectra (visible) obtained upon femtosecond flash photolysis (387 nm) of red-emitting CdTe, 5 nm, (1.0×10^{-6} M) with several time delays between 0 and 20 ps at room temperature. Lower part: time−absorption profiles of the spectra shown above at 500, 550, 585, and 650 nm.

these observations we must conclude that once photoexcited, CdTe undergo charge transfer to the electron-accepting SWNT or MWNT. The charge transfer is, however, masked by the instrument response time of around 100 ps.

To learn more about CNT/CdTe interactions, we turned to transient absorption measurements following either short femtosecond (i.e., at 387 nm) or long nanosecond (i.e., at 355 nm) photoexcitation. For red- and green-emitting CdTe we see that the time window of the first picosecond is dominated by the generation of an initial excited state. Characteristics of this state are transient bleaches of the transitions across the band gaps (i.e., red CdTe, at around 580 nm; green CdTe, at around 570 nm) and new peaks that are located in the red relative to the band gap transition (i.e., red CdTe, at 645 nm; green CdTe, at 635 nm). Figure 2 demonstrates that these states are metastable and that they decay with rates of $4.2 \pm 0.5 \times 10^{11}$ s^{-1} (red CdTe) and $3.3 \pm 0.5 \times 10^{11}$ s^{-1} (green CdTe)—as major components. Implicit is here that an equilibration of charge density occurs, as evidenced by a slight red-shift of the transient bleach. Once these equilibrated states are reached no significant decays are noted on the entire time scale of our experiments (i.e., up to 1500 ps). Upon extending the time scale into the nanosecond domain (i.e., starting at around 10 ns) we see (i) the same transient characteristics (see Figure S3 in the Supporting Information) and (ii) that they decay slowly ($\sim 3.5 \pm 0.5 \times 10^{7}$ s^{-1}) back to the ground state.

When investigating SWNT/pyrene^{+}/CdTe or MWNT/pyrene^{+}/CdTe (i.e., corresponding to the endpoint of our absorption and emission titrations) the same initial processes occur, vide supra. In contrast to the case of just CdTe alone, time−absorption profiles in Figure 3 indicate that a competing process interferes kinetically with the one that corresponds to the fast equilibration reaction. Spectroscopically, we also see a difference: new transient features develop that differ significantly from those registered for just CdTe (compare Figures 2 and 3). For example, for the case of red CdTe and MWNT new maxima develop at

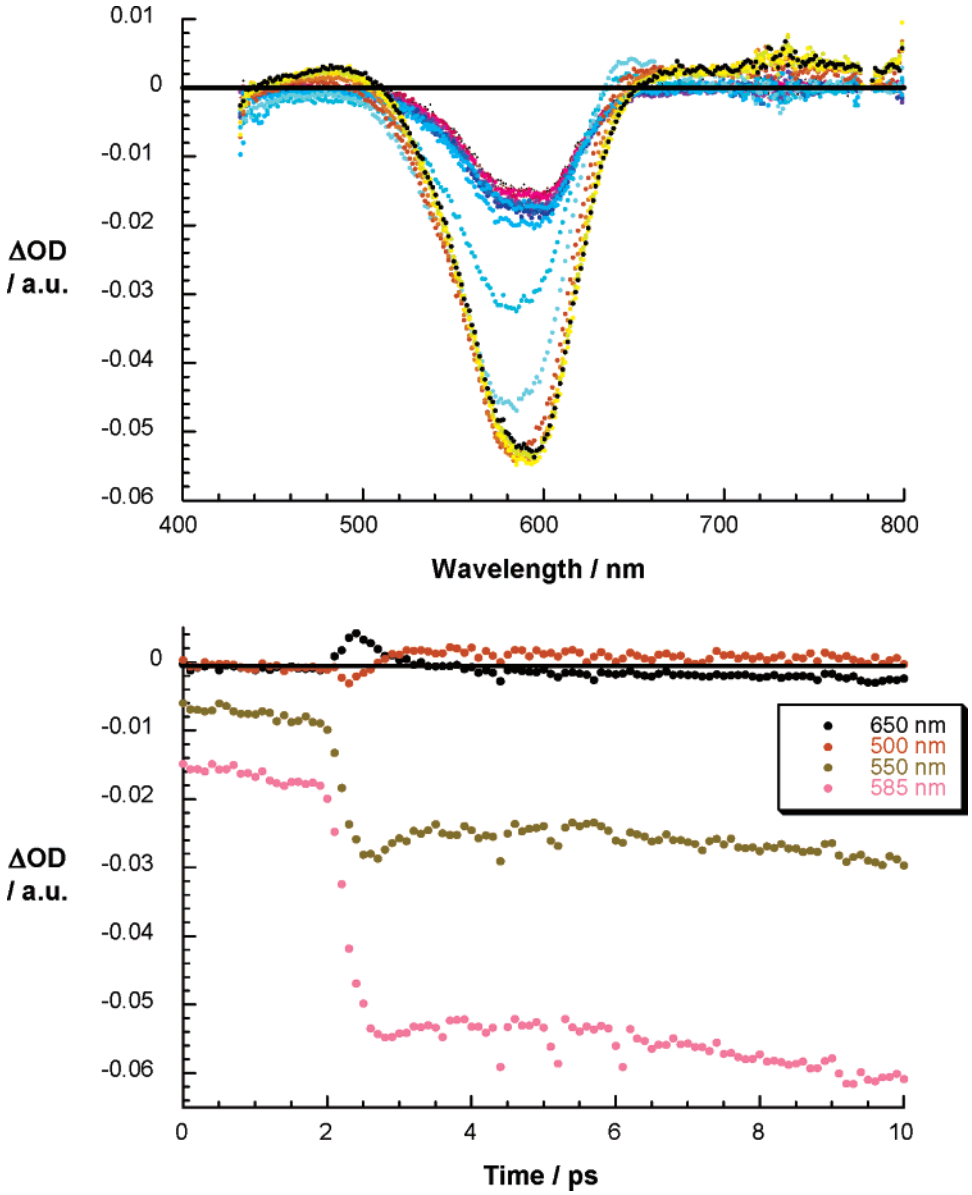

Figure 3. Upper part: differential absorption spectra (visible) obtained upon femtosecond flash photolysis (387 nm) of MWNT/pyrene^{+}/red-emitting CdTe, 5 nm, (1.0×10^{-6} M) with several time delays between 0 and 20 ps at room temperature. Lower part: time−absorption profiles of the spectra shown above at 500, 550, 585, and 650 nm.

480 and 725 nm. Figure 4 confirms that we see for MWNT/pyrene^{+}/CdTe even on the nanosecond time scale (i.e., >10 ns) the same transients with a minimum at 580 nm and maxima at 460 and 720 nm. A remarkably slow decay of $4.7 \pm 0.5 \times 10^{4}$ s^{-1} was derived from fitting wavelengths all throughout the visible and infrared region. In analogous experiments with SWNT instead of MWNT (see Figure S4 in the Supporting Information) a slightly larger decay rate constant of $7.6 \pm 0.5 \times 10^{4}$ s^{-1} was determined.

A likely rationale for the transient changes implies charge transfer evolving from the photoexcited electron donor (i.e., CdTe) to the electron acceptor (i.e., SWNT or MWNT). To find spectroscopic proof for this hypothesis we turned to pulse radiolytic oxidation (i.e., $Br_2^{\bullet -}$)[18] and reduction (i.e., hydrated electrons)[18] experiments with CdTe and SWNT/pyrene^{+} or

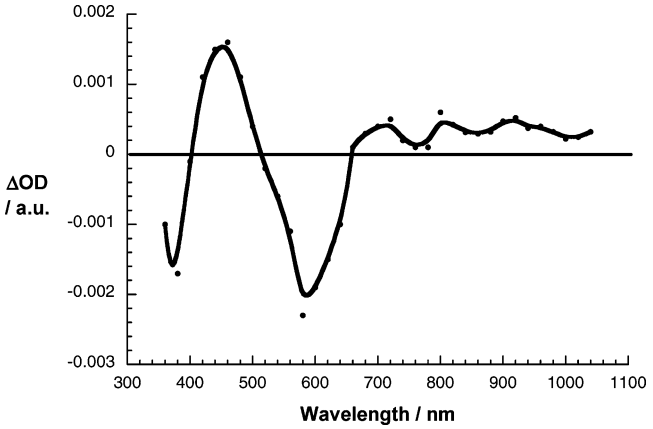

Figure 4. Differential absorption spectrum (visible and near-infrared) obtained upon nanosecond flash photolysis (355 nm) of MWNT/pyrene^{+}/red-emitting CdTe, 5 nm, (1.0×10^{-6} M) with a time delay of 50 ns at room temperature.

(18) For details on the pulse radiolytic experiments see: *Radiation Chemistry: Present Status and Future Trends*; Jonah, C. D., Rao, B. S. M., Eds.; Elsevier: Amsterdam, 2001.

CdTe and MWNT/pyrene$^+$, respectively. Spectral attributes of oxidized CdTe are a minimum at 590 nm and maxima at 460 nm/730 nm—well in line with the features shown in Figures 4 and S4 in the Supporting Information. Figure S5 in the Supporting Information, on the other hand, shows that the reduction of SWNT/pyrene$^+$ with hydrated electrons consists of two contributions, that is, reduction of pyrene$^+$ (i.e., 800 nm maximum) and reduction of SWNT (i.e., a series of minima at 710, 880, 960, and 1040 nm). Please compare the latter values with minima at 740, 870, 940, and 1020 nm as they were seen in the spectra that were photolytically generated. Informative tests came from separate reduction experiments with SWNT−PSS (i.e., a water-soluble SWNT grafted with poly(sodium 4-styrenesulfonate)) and pyrene$^+$.[19] In conclusion, the transient absorption spectra are composite spectra of oxidized CdTe and reduced SWNT/MWNT features and resemble the photoreactivity seen for CdTe associated with water-soluble fullerene derivatives.[16]

It is also important to note that the choice of CdTe over other available nanocolloids was not random. CdTe is a lot more reactive than CdSe or CdS and has substantial electron-donor activity that matches electron-acceptor characteristics of CNTs. Encouraged by such remarkable features we pursued the use of CNT and CdTe as integrative components for photoelectrochemical hybrid cells. In this light, we modified ITO electrodes with a base layer of polyelectrolytes (i.e., poly(diallyl-dimethylammonium) chloride (PDDA) or sodium poly(styrene-4-sulfonate) (PSS)) following the technique of layer-by-layer (LBL) assembly that we often used in the past.[20] Their hydrophilic headgroups provide multipoint interactions with charged entities via uniformly directed Coulombic forces and short-range van der Waals forces. In addition to these forces, charge-transfer attractions between the components are expected to be strong for CNT/CdTe systems based on the results described above. Before LBL coating, all substrates in this study—quartz slides (for absorption measurements), silicon wafers (for AFM measurements), and ITO electrodes (for photoelectrochemical measurements)—were purified in piranha solutions for 1 min. Bilayers made from SWNT/pyrene$^+$ and CdTe were deposited onto the polyelectrolyte base layers. Important is that the ITO/SWNT/CdTe sequence creates a redox gradient, namely, facilitating electron mediation, starting from photoexcited CdTe to SWNT and, finally, to ITO. Recent work suggests that assemblies with electronic gradients enhance the charge-transfer reactions.[15h]

Absorption spectroscopy, atomic force microscopy (AFM), and scanning electron microscopy (SEM) are powerful ways to monitor the individual deposition steps. In Figure S6 in the Supporting Information, typical absorption spectra of the photo- and electroactive species are shown—quartz was used as a substrate to allow transparency below 375 nm. Discernible are the SWNT van Hove singularities (i.e., all throughout the spectrum) and the band gap transition in CdTe, while the polyelectrolyte layers do not absorb significantly in the 300−900 nm region. This supports the notion that all components were successfully integrated during the deposition procedure and CNT exist primarily in the form of single strands rather than bundles which is attributed to the effective solubilization by pyrene compound. AFM and SEM—performed with CNT/pyrene$^+$ and CNT/pyrene$^+$/CdTe-coated silicon wafers—back up this conclusion. While the polyelectrolyte base layers are essentially featureless, CNT give rise to densely covered surfaces, showing in most cases the presence of individual SWNT and MWNT. Figure 5 shows SEM images of MWNT/pyrene$^+$ with different magnifications. The surface is clearly covered with CNT and CdTe in the AFM images (Figure 6). We can see that, in our topographic investigation, also the voids between CNT are filled with CdTe, due to adhesion to the polyelectrolyte surface. Note also the tight contact between the CND and the CdTe nanoparticles which completely surround them, producing a closely packed assembly.

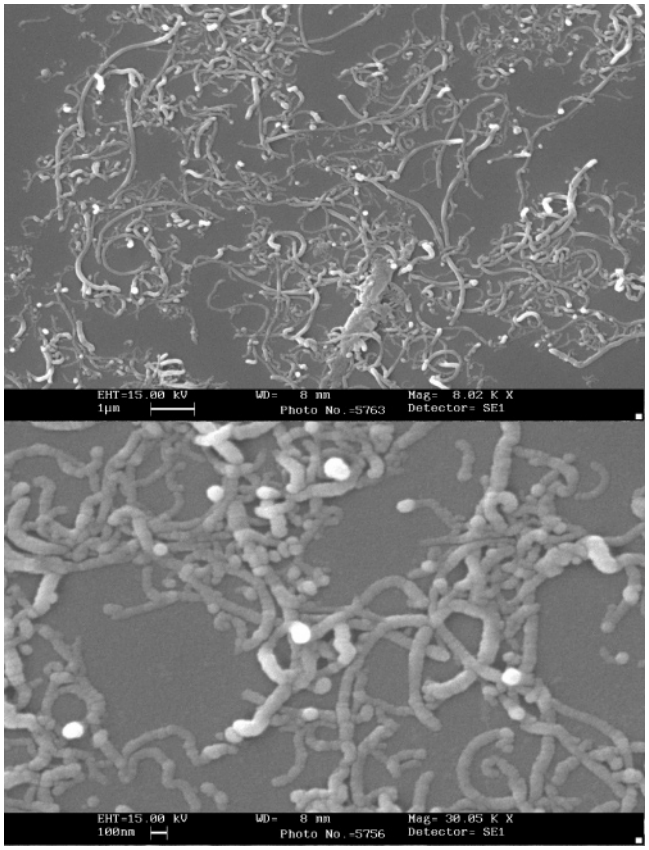

Figure 5. SEM images of MWNT/pyrene$^+$ on silicon wafers with different magnifications.

Immediately after their preparation CNT/pyrene$^+$ and CNT/pyrene$^+$/CdTe hybrid cells were immersed into aqueous solutions (i.e., 0.1 M Na_3PO_4, 1 mM sodium ascorbate, N_2-purged) with a Pt cathode connected externally to the ITO anode to measure the photocurrents. First the photocurrents were tested as a function of incident photon flux. For most of the correlation (i.e., 200−500 W) a linear dependence was noted, which led

(19) In the photolytic experiments pyrene$^+$ is not involved in the electron-transfer character.

(20) (a) Decher, G.; Hong, J. D. *Ber. Bunsen-Ges. Phys. Chem.* **1991**, *95*, 1430. (b) Ferreira, M.; Cheung, J. H.; Rubner, M. F. *Thin Solid Films* **1994**, *244*, 806. (c) Keller, S. W.; Kim, H. N.; Mallouk, T. E. *J. Am. Chem. Soc.* **1994**, *116*, 8817. (d) Lvov, Y.; Decher, G.; Haas, H.; Mohwald, H.; Kalachev, A. *Physica B* **1994**, *198*, 89. (e) Kotov, N. A. *Nanostruct. Mater.* **1999**, *12*, 789. (f) Dubas, S. T.; Schlenoff, J. B. *Macromolecules* **1999**, *32*, 8153. (g) Hammond, P. T. *Curr. Opin. Colloid Interface Sci.* **2000**, *4*, 430. (h) Durstock, M. F.; Taylor, B.; Spry, R. J.; Chiang, L.; Reulbach, S.; Heitfeld, K.; Baur, J. W. *Synth. Met.* **2001**, 116. (i) Yoo, S.; Shiratori, S. S.; Rubner, M. F. *Macromolecules* **1998**, *31*, 4309. (j) Kotov, N. A.; Fendler, J. H.; Dekany, I. *J. Phys. Chem.* **1995**, *99*, 13065−13069. (k) Mamedov, A. A.; Kotov, N. A.; Prato, M.; Guldi, D.; Wicksted, J. P.;Hirsch, A. *Nat. Mater.* **2002**, *1*, 190−194. (l) Olek, M.; Ostrander, J.; Jurga, J.; Möhwald, H.; Kotov, N. A.; Kempa, K.; Giersig, M. *Nano Lett.* **2004**, *4*, 1889−1895.

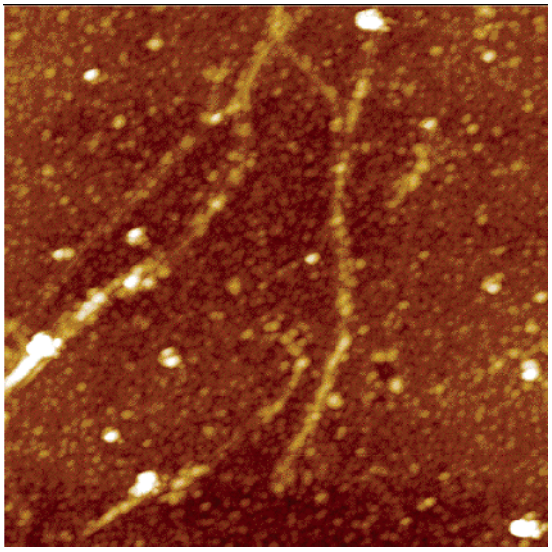

Figure 6. AFM image of SWNT/pyrene$^+$/red-emitting CdTe, 5 nm, on a silicon wafer; the scan area is 1.5 μm × 1.5 μm.

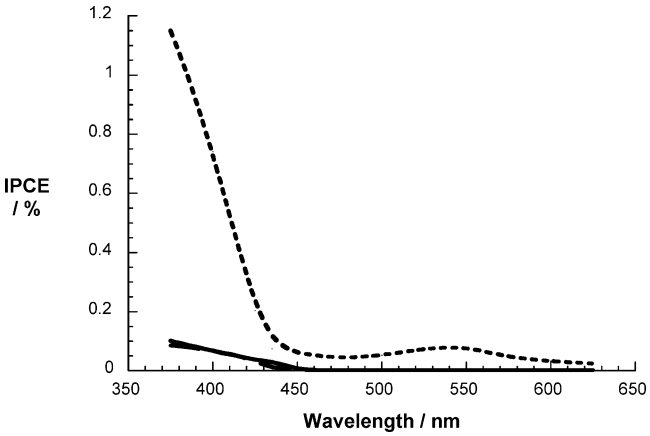

Figure 7. Photoaction spectra of SWNT/pyrene$^+$ (full line), MWNT/pyrene$^+$ stack (dashed line), and SWNT/pyrene$^+$/red-emitting CdTe stack (dotted line). Experimental conditions: 0.1 M Na_3PO_4, 1 mM sodium ascorbate, N_2-purged, no electrochemical bias.

us to use 400 W in our experimental work.[13c] When the cells are illuminated with visible light distinct photocurrent patterns develop. For CNT/pyrene$^+$, that is, in the absence of CdTe, in good agreement with the absorption spectra photoaction spectra evolved (Figure 7) that showed a maximum light response around 375 nm, combined with a moderately low monochromatic internal photoconversion efficiency (IPCE) of about 0.1% in the presence of 1mM ascorbate. These trends suggest that the electron transfer into the ITO conduction band evolves from the one-electron reduced state of CNT and also from their photoexcited states.

The photocurrents (Figure 7) were appreciably higher after adding CdTe.[21] For example, under white light illumination we see for SWNT/pyrene$^+$/red CdTe and SWNT/pyrene$^+$/green CdTe 11.5- and 7.2-fold amplification of the photocurrent, relative to the photocurrents seen without CdTe. A smaller amplification factor, as seen for green-emitting CdTe, 3.5 nm, relates to poorer light harvesting features in the visible range—compare the band gap transitions in red- and green-emitting

(21) When monitoring several back-to-back intervals of light-on and light-off, exceptionally reproducible and stable photocurrents were obtained.

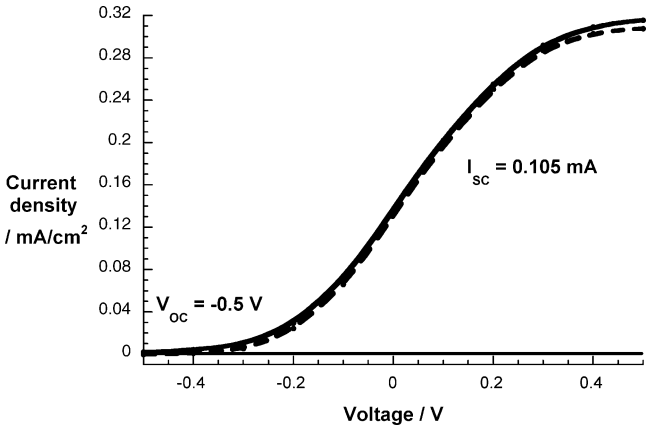

Figure 8. *I*–*V* characteristics of a single SWNT/pyrene$^+$/red-emitting CdTe stack under white light illumination: 0.1 M Na_3PO_4, 1 mM sodium ascorbate, N_2-purged.

CdTe. As well the lower position of the valence band in CdTe of smaller size makes these particles less potent electron donors, and thus, such assemblies are less efficient than red-emitting nanoparticles in producing a charge-separated state. Photoaction spectra, as depicted in Figure 7, clearly identify the CdTe as the major photoactive species and match the absorption spectra. In particular, both UV regions, maximizing around 375 nm, and visible regions, centered around 550 nm, correlate well with the absorption spectra shown in Figure S1 in the Supporting Information. In the case of SWNT/pyrene$^+$, the monochromatic IPCE values for red- and green-emitting CdTe are 1.15% and 0.72%, respectively.

From our experiments we derive the following photocurrent mechanism: Photoexcitation of CdTe is followed by rapid interactions with CNT leading to a sequential electron injection into SWNT and ITO. Notably, CNT are likely to act as charge delivery channels, rapidly transporting the charge carriers from the photogeneration point to the electrode. Ascorbate, on the other hand, helps to regenerate the CdTe ground state—some photooxidation of CdTe is likely to occur regardless of the presence of ascorbate. Finally, when comparing SWNT- and MWNT-based cells, we note a 1.2-times higher light efficiency for the MWNT system (i.e., 1.4%). Overall, these values compare well with our previous reports on SWNT/pyrene$^+$/polythiophene and SWNT/pyrene$^+$/ZnP.[8–13c,l]

Additional proof for the proposed mechanism came from current–voltage characteristics, in which we probed CNT/pyrene$^+$/red CdTe and red CdTe/CNT/pyrene$^+$ cells in a potential range between −0.5 V and +0.5 V.[22,23] Figure 8 exemplifies the behavior for SWNT/pyrene$^+$/red CdTe. Under open circuit voltage conditions the acceptor level of SWNT is in equilibrium with the conducting band of ITO, and the electron flow is blocked. From this point the photocurrent increases systematically toward the positive potentials. Increased charge separation and facilitated transport of charge carriers under positive bias are responsible for the enhanced photocurrent generation. At a bias of +0.5 V the IPCE corresponds to 2.3% (i.e., SWNT/pyrene$^+$/red CdTe). For red CdTe/CNT/pyrene$^+$/ cells a trend is noted (see Figure S7 in the Supporting

(22) Photoaction spectra of red CdTe and red CdTe/CNT/pyrene$^+$ cells are identical to that shown for SWNT/pyrene$^+$/red CdTe in Figure 7.

(23) A SWNT/pyrene$^+$/red CdTe cell is about 6-times more efficient than a red CdTe cell (Figure S8 in the Supporting Information), measured with absorptions that are typically 1.5-times stronger in the 350–550 nm range.

Scheme 2. Cartoon that Exemplifies the Working Mode of CNT/Pyrene$^+$/Red CdTe (i.e., Case I) and Red CdTe/CNT/Pyrene$^+$ (i.e., Case II) Hybrid Cells

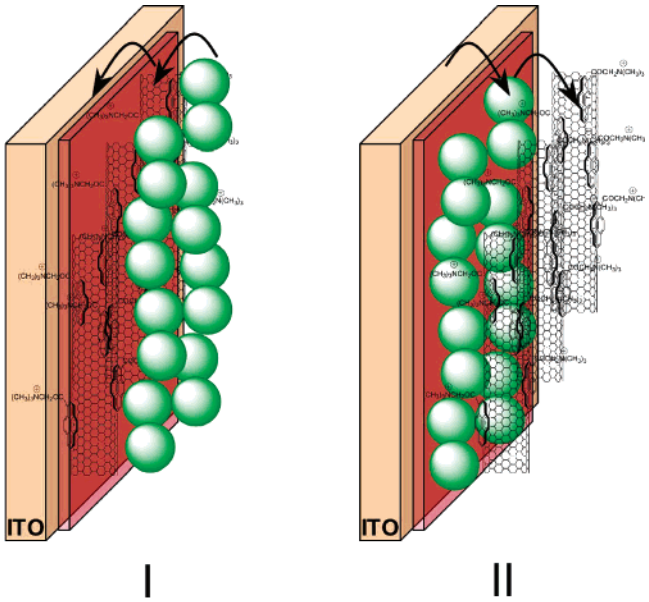

Information) that prompts to an electron flow that is reversed. Initial charge separation within red CdTe/CNT/pyrene$^+$ is followed by hole injection into the ITO electrode. Applying a negative bias at the ITO electrode surface is expected to facilitate the hole injection from the oxidized electron donor. In fact, changing the bias from −0.5 V and +0.5 V leads to a steady decrease of the photocurrent.

Conclusions

To conclude, organic (CNT) inorganic (CdTe) nanohybrids were systematically devised and tested as donor−acceptor nanohybrids in dilute condensed media and as integrative components at electrode surfaces. Strong electronic interactions in the ground and excited state are responsible for favorable charge-transfer characteristics. Subsequently, electrostatic and van der Waals interactions, between the individual components (i.e., polyelectrolyte, CNT/pyrene$^+$, and CdTe), have been employed for the sequential integration of photoactive layers into novel hybrid cells. In response to visible light irradiation, appreciable photoelectrochemical device performances were registered. Important is that depending on the sequence of deposition, namely, CNT/pyrene$^+$/red CdTe or red CdTe/CNT/pyrene$^+$, the photocurrent mechanism is altered, as Scheme 2 demonstrates.

Highest monochromatic IPCEs, of up to 2.3%, were registered for hybrid cells consisting of single SWNT/pyrene$^+$/red-emitting CdTe stacks. Considering the simplicity and universality of our approach, combined with the useful efficiency found for single stack coverages, we believe we have demonstrated a potent alternative in fabricating photoactive molecular devices. Currently, we are exploring and fine-tuning critical features, such as improved charge carriers and/or redox gradient, within multistack LBL nanoconstructs.[24]

Experimental Section

Synthesis. Preparation of CNT·pyrene$^+$: Water-soluble SWNTs were obtained in analogy to previous work, using 1-(trimethylammonium acetyl) pyrene (pyrene$^+$). However, to reduce the amount of free pyrene in solution, the SWNT/pyrene$^+$ complex was allowed to precipitate, and the centrifuged solid was resolubilized in water. The same procedure was applied to prepare MWNT• pyrene$^+$. Green (2.4 nm), yellow (3.4 nm), and red (5.0 nm) CdTe were synthesized following well-known protocols.[4]

Photophysics. Femtosecond transient absorption studies were performed with 387 nm laser pulses (1 kHz, 150 fs pulse width) from an amplified Ti:Sapphire laser system (model CPA 2101, Clark-MXR Inc.). Nanosecond laser flash photolysis experiments were performed with 532 nm laser pulses from a Quanta-Ray CDR Nd:YAG system (6 ns pulse width) in a front face excitation geometry. Fluorescence lifetimes were measured with a Laser Strobe fluorescence lifetime spectrometer (Photon Technology International) with 337 nm laser pulses from a nitrogen laser fiber-coupled to a lens-based T-formal sample compartment equipped with a stroboscopic detector. Details of the Laser Strobe systems are described on the manufacture's web site. Emission spectra were recorded with a SLM 8100 spectrofluorometer. The experiments were performed at room temperature. Each spectrum represents an average of at least five individual scans, and appropriate corrections were applied whenever necessary.

Pulse Radiolysis. Pulse radiolysis experiments were performed using 50 ns pulses of 15 MeV electrons from a linear electron accelerator (LINAC). Details of the equipment and the data acquisition have been described elsewhere.[25] Dosimetry was based on the oxidation of SCN^- to $(SCN)_2^{\bullet -}$ which in aqueous, N_2O-saturated solution takes place with $G \approx 6$ (G denotes the number of species per 100 eV, or the approximate μM concentration per 10 J of absorbed energy). The radical concentration generated per pulse was varied between $(1-3) \times 10^{-6}$ M.

Film Preparation. A 1% solution of PDDA, pH = 8.5 and DI water for rinsing, pH = 7.2 were used. All solutions were made in DI water/phosphate buffer. Silicon wafers, ITO, and quartz slides were cleaned in piranha solution, rinsed with DI water, sonicated for 15 min and again thoroughly rinsed with DI water. After that, they were coated with a precursor layer of PDDA (10 min exposure), followed by deposition of SWNT·pyrene$^+$ and CdTe (60 min exposure).

Photoelectrochemical Measurements. Photoelectrochemical measurements were carried out in a three-arm cell that had provision to insert a working electrode (ITO), counter (Pt gauze), and reference Ag/AgCl (KCl 0.1 M) (when bias voltage was applied). The electrolyte was 0.1 M Na_3PO_4 and either N_2 or O_2 was bubbled into the solution for 10−15 min prior to photoelectrochemical measurements. The voltage was applied using a Princeton Applied Research, model 175 galvanostat/potentiostat. Photocurrent measurements were carried out using a two-electrode Keithley model 617 programmable electrometer immediately after illumination. A collimated light beam from a 150 W xenon lamp was used for UV illumination. When white light was used, a 375 nm cut filter was used. When recording a photoaction spectrum, a Bausch and Lomb high-intensity grating monochromator was introduced into the path of the excitation beam for selecting the required wavelengths. The incident photon to current conversion efficiency (IPCE), defined as the number of electrons collected per incident photon, was evaluated from short circuit photocurrent measurements at different wavelengths versus the photocurrent measured using a photodiode of the type PIN UV 100 (UDT Sensors Inc.).

Acknowledgment. This work was carried out with partial support from the EU (RTN network "WONDERFULL"), MIUR (PRIN 2004, prot. 2004035502), SFB 583, and the Office of Basic Energy Sciences of the U.S. Department of Energy. This

(24) Mamedov, A. A.; Belov, A.; Giersig, M.; Mamedova, N. N.; Kotov, N. A. *J. Am. Chem. Soc.* **2001**, *123*, 7738−7739.

(25) Hug, G. L.; Wang, Y.; Schöneich, C.; Jiang, P.-Y.; Fessenden, R. W. *Radiat. Phys. Chem.* **1999**, *54*, 559.

is Document NDRL-4643 from the Notre Dame Radiation Laboratory.

Supporting Information Available: Absorption spectra, fluorescence spectra, differential absorption spectra, photoactive current spectra, and $I-V$ characteristics. This material is available free of charge via the Internet at http://pubs.acs.org.

JA0550733